Journal of Catalysis 278 (2011) 246–252

Contents lists available at ScienceDirect

Journal of Catalysis

journal homepage: www.elsevier.com/locate/jcat

Shape-selective synthesis of methylamines over the RRO zeolite Al-RUB-41

Bart Tijsebaert [a], Bilge Yilmaz [b], Ulrich Müller [b], Hermann Gies [c], Weiping Zhang [d], Xinhe Bao [d], Feng-Shou Xiao [e], Takashi Tatsumi [f], Dirk De Vos [a,*]

[a] Centre for Surface Chemistry and Catalysis, K.U.Leuven, Kasteelpark Arenberg 23, 3001 Leuven, Belgium
[b] BASF AG, GCC/Z M 301, Ludwigshafen, Germany
[c] Institute für Geologie, Mineralogie und Geophysik, Ruhr-Universität Bochum, Germany
[d] State Key Laboratory of Catalysis, Dalian, China
[e] State Key Laboratory of Inorganic Synthesis and Preparative Chemistry, Jilin University, Changchun, China
[f] Tokyo Institute of Technology, Yokohama, Kanagawa, Japan

ARTICLE INFO

Article history:
Received 10 September 2010
Revised 8 December 2010
Accepted 16 December 2010
Available online 28 January 2011

Keywords:
Methylamine synthesis
Amination
Catalysis
Zeolite
Synthesis
Layered materials
Monomethylamine
Dimethylamine
Ammonia

ABSTRACT

Aluminum was incorporated into the layered silicate RUB-39, which is transformed by calcination into RUB-41. This new zeolite with RRO topology contains 8- and 10-ring pores, and the acid sites in the aluminated material catalyze the synthesis of methylamines, in particular mono- and dimethylamine, by amination of methanol. Owing to the shape-selective catalytic properties of (H)Al-RUB-41, low selectivity to the thermodynamically favored trimethylamine product is obtained in comparison with results on RUB-39 or non-shape-selective materials. Both activity and selectivity are highest for RUB-41 catalysts with a high Si to Al ratio. Silylation reduces the number of unselective sites and results in a further suppression of trimethylamine formation. The introduction of acidity in the intact RUB-41 structure is supported by Al-MAS NMR and NH_3-TPD data. Additional characterization by XRD and SEM is provided.

1. Introduction

Zeolites are widely used as heterogeneous catalysts in the chemical industries for the production of petrochemicals, fine chemicals, etc. Their high surface area, well-defined pore structure, and tunable acidity constitute an appropriate basis to catalyze a broad scope of transformation processes. As each process requires different types of catalysts and because of the permanent quest for more sustainable catalytic processes, there are constant efforts to develop new zeolite materials with improved catalytic properties, for example, resulting in higher product selectivities [1].

Recently, innovative synthesis pathways have been developed wherein layered silicates are transformed into three-dimensional silicate frameworks. For example, zeolites like MWW [2], EU-20b [3], CDS-1 [4], Nu-6(2) [5], and RWR [6] were synthesized by conversion of the layered silicates ERB-1 [2], EU-19 [3], PLS-1 [4], Nu-6(1) [5], and RUB-18 [6]. Similar research led to the development of the all-silica RUB-41 zeolite with RRO topology starting from the layered material RUB-39. After the topotactic layer condensation to RUB-41, a two-dimensional pore system is created in between the layers. The pore system comprises intersecting 8- and 10-membered ring pores. From structure analysis, their dimensions are determined as 5.8 Å × 4.1 Å (8MR) and 5.9 Å × 4.1 Å (10MR) [7]. In previous work, we demonstrated the selective adsorption of 2-butenes out of a mixture of the four butene isomers on such an all-silica RUB-41 zeolite. *Trans*-2-butene, with a critical diameter of 0.431 nm, and *cis*-2-butene, with a critical diameter of 0.494 nm, were preferred in the adsorption over 1-butene and isobutene. This selectivity was ascribed to the distorted 10-rings present in RUB-41 [8] and suggests that the effective diameter of these 10-rings is hardly larger than that of the 8-ring windows.

In the present work, aluminum was introduced into the RUB-41 structure via various routes, which results in a catalytically active aluminosilicate material. As a test reaction, (H)Al-RUB-41 was employed in the synthesis of methylamines from methanol and ammonia. Methylamines are widely used intermediates in the synthesis of fine and specialty chemicals, for instance in the synthesis of pharmaceuticals (e.g., theophylline), pesticides, or surfactants. In the methanol amination reaction, monomethylamine (MMA), dimethylamine (DMA), trimethylamine (TMA), and water are the typical reaction products [9]. The thermodynamic equilibrium

* Corresponding author.
E-mail address: dirk.devos@biw.kuleuven.be (D. De Vos).

0021-9517/$ - see front matter © 2010 Elsevier Inc. All rights reserved.
doi:10.1016/j.jcat.2010.12.010

and thus product distribution are controlled by the ratio of ammonia versus methanol as well as by the reaction temperature. For thermodynamic reasons, TMA is predominantly formed, but the demand for monomethylamine and dimethylamine is much higher. Therefore, an ammonia excess and a recycle of undesired TMA are often applied in the process. However, this approach requires expensive purification steps, also because of the azeotropic mixtures intermediately formed. To overcome these limitations, shape-selective catalysts have been introduced [10].

The first commercially available shape-selective catalysts were applied by Nitto and consisted of a mordenite treated with tetraethoxysilane to enhance the selectivity to the mono- and dialkylated amines [11]. A large body of further work focused on the shape-selective properties of small pore zeolites containing typically cages that can be accessed via 8-membered ring pore windows [12–19]. Active and selective amination catalysts are for instance H-Rho, H-chabazite, and H-levyne zeolites. The windows of the cages in these materials are sufficiently small to prevent the egress of trimethylamine.

In this work, we report on the activity and shape-selective properties of (H)Al-RUB-41 in methanol amination. As is apparent from the literature background, this reaction is a sensitive one to detect even minor amounts of non-selective sites. Important questions are whether the RUB-41 pore system of 8-rings and distorted 10-rings may allow shape-selective methanol amination and whether the Al-siting can be controlled so as to mostly generate active sites only in a shape-selective environment. The effect of aluminum content on selectivity and conversion and the influence of post-synthesis modification by a silylating agent will also be investigated.

2. Experimental

2.1. Catalyst preparation

Different Al-RUB-41 materials with varying Al content were synthesized. Typically, the molar composition of the synthesis gel in the first step was 1 SiO_2: 0.5 SDA: 0–0.08 NaOH: 2–10 H_2O. Dimethyldipropylammoniumhydroxide was used as structure-directing agent (SDA). After aging of the gel for 1 h at room temperature, it was kept in Teflon-lined stainless steel autoclaves and stirred at a temperature of 140 or 150 °C at 15 rpm for 2–4 days. Seeding crystals of RUB-39 were added to shorten crystallization times. After this first stage, the synthesis mixture was cooled, and a minute amount of Al isopropoxide or $NaAlO_2$ was added to the gel. This was carried out using synthesis mixtures with SiO_2/Al_2O_3 = 30–200 and SiO_2/SDA = 2.

Crystallization was continued for another 2–4 days. The as-synthesized, layered Al-RUB-39 material was converted to Al-RUB-41 by slow heating at 1 °C/min until 520 °C in a furnace under static air. After 12 h at this temperature, heating was continued until 560 °C for 4 h.

To eliminate any Na^+ that could be present as a residue from the synthesis, samples were three times ion-exchanged in a solution of 0.5 M NH_4NO_3 at 80 °C for 24 h and washed with distilled water. Next, these samples were dried at 70 °C and calcined for 6 h in a furnace under static air with a constant temperature increase of 1 °C/min from 20 °C to 450 °C. Silylation was performed with a hexamethyldisilazane (HMDS) treatment. One gram of the calcined(H)Al-RUB-41 catalyst was dried at 200 °C and added to a solution of 0.38 g HMDS in 10 g toluene. The resulting mixture was refluxed under N_2 atmosphere at 120 °C for 2 h. The silylated sample was filtered, abundantly washed with toluene, and subsequently dried at 70 °C [20]. A sample designation list can be found in Table 1. Al-RUB-41 could be synthesized with different Si/Al ratios. Samples A1–A4 were synthesized using aluminum isopropoxide; sample B was synthesized using sodium aluminate.

Table 1
Overview of Al-RUB-41 samples employed.

	Al source	Si/Al	BET (m^2/g)	NH_3 mmol g^{-1} adsorbed
A1	Al isopropoxide	19	69	0.413
A2	Al isopropoxide	25	412	0.285
A3	Al isopropoxide	51	350	0.156
A4	Al isopropoxide	163	323	0.062
B	Sodiumaluminate	20	270	0.218

ZSM-5 CBV 2314 was obtained from ZEOLYST and has a Si/Al ratio of 20. A chabazite sample (Si/Al = 16) was obtained from BASF Ludwigshafen. XRD showed the pattern of pure and fully crystalline chabazite (checked as-synthesized and after ion exchange). FE-SEM analysis showed the typical cube morphology. Al-MCM-41 (Si/Al = 10) was synthesized according to a modified Stoeber method [21].

2.2. Characterization

^{27}Al MAS NMR spectra of the samples were acquired on a Varian Infinity Plus-400 spectrometer at 104.2 MHz using a 4 mm MAS NMR probe head with a spinning rate of 10 kHz. Chemical shifts were referenced to $(NH_4)Al(SO_4)_2{\cdot}12H_2O$ at −0.4 ppm as a secondary reference. All spectra were accumulated for 12,000 scans with a $\pi/4$ flip angle and a 2-s pulse delay. The X-ray powder diffraction analysis was carried out with a Siemens 5000D diffractometer using CuKα radiation (λ = 0.15401 nm). Nitrogen adsorption isotherms were determined by physisorption of nitrogen at 77 K on a Coulter Omnisorp 100 CX. Prior to measurements, the samples were outgassed under vacuum at 473 K overnight. SEM micrographs were recorded using a Philips XL30 FEG. The temperature-programmed desorption of ammonia (NH_3-TPD) experiments were performed using a Micromeritics AutoChem II 2920 automated chemisorption analysis unit with a thermal conductivity detector (TCD) under helium flow. The sample was heated with a temperature ramp of 20 °C/min–500 °C under He flow. After staying at that temperature for 10 min, it was cooled down to 100 °C in He atmosphere. Ammonia saturation was carried out at 100 °C using a 10% NH_3–He gas mixture. After saturation, excess ammonia was purged from the chamber under flowing He at 100 °C for 1 h. The desorption step was performed with a temperature ramp of 10 °C/min up to 500 °C under He flow. Desorbed species were observed with the on-line mass spectroscopy unit, which confirmed that the TCD signal indeed corresponded to ammonia desorption.

2.3. Catalytic experiments

Catalytic experiments were performed in a continuous flow fixed-bed reactor. Prior to reaction, 200 mg of calcined zeolite sample in the H^+-form was pelletized. Pelletizing was done by pressing the catalyst between 2 iron bolts at 200 bar followed by sieving to obtain the 250–500 μm fraction. Then, the catalyst was pretreated in the reactor at 400 °C under a helium flow of 5.6 mL/min. Thereafter, the reactor was cooled to reaction temperature (300 or 340 °C). The reaction was carried out by feeding the reactor with a 1:1 or a 2:1 mixture (on mole basis) of ammonia and methanol diluted in helium. Methanol was fed to the reactor by passing a helium flow through a methanol-filled saturator. Mass flow controllers enabled to adjust the ammonia to methanol ratio. Typically, the gas flow of a 2:1 mixture contained 1.6 mL/min NH_3 and 5.6 mL/min MeOH+He, or reactant partial pressures of 22.5 kPa NH_3 and 11.25 kPa MeOH, which resulted in a WHSV of 0.66 g_{feed} $g^{-1}_{catalyst}$. For a 1:1 mixture, gas flows of 0.8 mL/min NH_3 and

5.6 mL/min MeOH+He were used which resulted in a WHSV of 0.49 $g_{feed}\ g^{-1}_{catalyst}$. The outlet was analyzed by a HP 5890 series II gas chromatograph equipped with a WCOT fused silica 60 m column.

3. Results and discussion

3.1. Catalyst characterization

Characterization by SEM, NMR, XRD, and TPD revealed the formation of an aluminum containing RUB-41. Fig. 1 shows a typical SEM picture, in this case of Al-RUB-41 sample A4. The Al-RUB-41 structure consists of thin layers that condense upon calcination, which results in colorless crystals with a platy morphology. The crystal dimensions are about 5–10 μm in diameter and <1 μm in thickness. This morphology is analogous to that of siliceous RUB-41, proving that the presence of Al does not have a major impact on the growth of the crystallites.

The RRO structure of the RUB-41 samples is evidenced by their X-ray diffractograms (Fig. 2). The diffraction patterns of Al-RUB-39, Al-RUB-41, and the all-silica analogues were recorded. The XRD pattern of the Al-RUB-41 sample shows a highly crystalline structure with diffraction peaks corresponding to the RRO topology. No peaks pointing to the presence of impurities, e.g., of MFI, could be discerned, as characteristic MFI peaks, e.g., the pair of peaks at 8.9 and 9.1° 2θ are lacking.

Solid-state NMR is a powerful tool for characterizing the structure of zeolites, and in particular substitution by heteroatoms. Species with different coordination environments can be distinguished in ^{27}Al MAS NMR spectra as shown in Fig. 3. The signal at 54 ppm is assigned to framework tetrahedral aluminum, and the other one at about 0 ppm is attributed to the octahedral aluminum in the samples [22–24]. ^{27}Al MAS NMR spectra indicate that the framework Al is dominant in all samples.

In order to study the acidity of the Al-RUB-41 zeolites, a temperature-programmed desorption of adsorbed NH_3 was performed on samples A1 (Si/Al = 19), sample A2 (Si/Al = 25), sample A3 (Si/Al = 51), sample A4 (Si/Al = 163), and sample B (Si/Al = 20) (Fig. 4). The NH_3-TPD of samples A3 and A4 gives a maximum for the strong acid sites at 391 °C and 355 °C, respectively, whereas for the other materials, the maximum is at 314 °C for A1 or even absent for A2. Hence, the samples with a low aluminum content (A3 and A4) have stronger acid sites. The NH_3-TPD of sample B, synthesized out of sodium aluminate, shows desorption maxima at 182 °C and 347 °C.

3.2. Catalytic experiments

3.2.1. Methanol amination

In the methanol amination, the catalytic activity and product selectivity were measured for an Al-MCM-41 sample (Si/Al = 10),

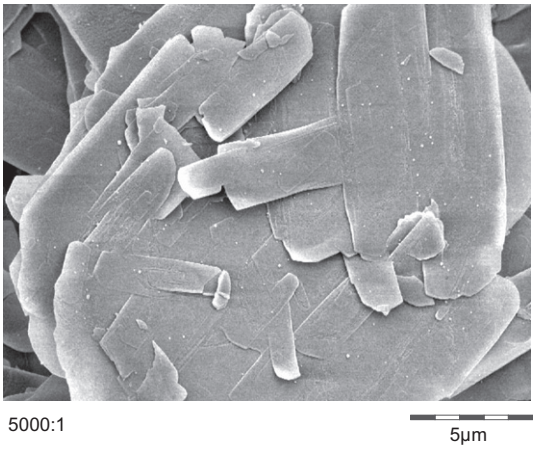

Fig. 1. SEM micrograph of Al-RUB-41 sample A4.

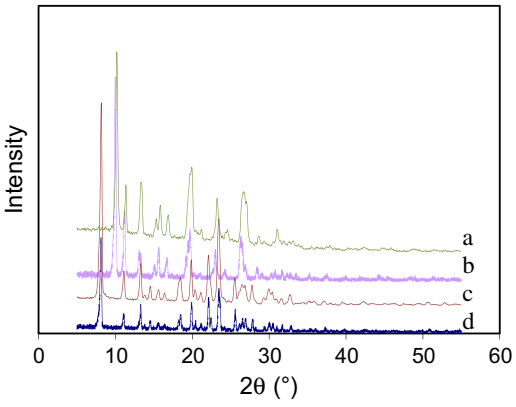

Fig. 2. X-ray diffraction patterns of (a) Al-RUB-41 (sample A3), (b) all-silica RUB-41, (c) Al-RUB-39 (precursor to sample A3), (d) all-silica RUB-39. The shift of the first diffraction line between RUB-39 and RUB-41 is due to condensation upon calcination.

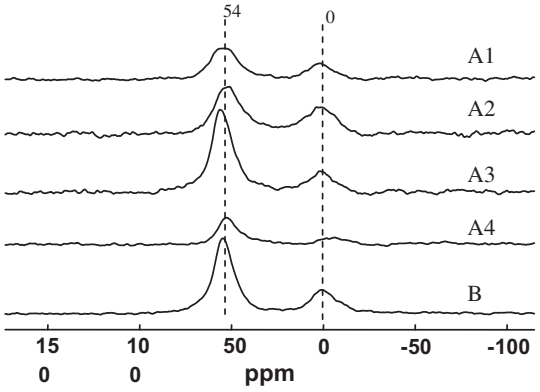

Fig. 3. Al MAS NMR spectra of Al-RUB-41 samples. Framework aluminum is dominant in all samples.

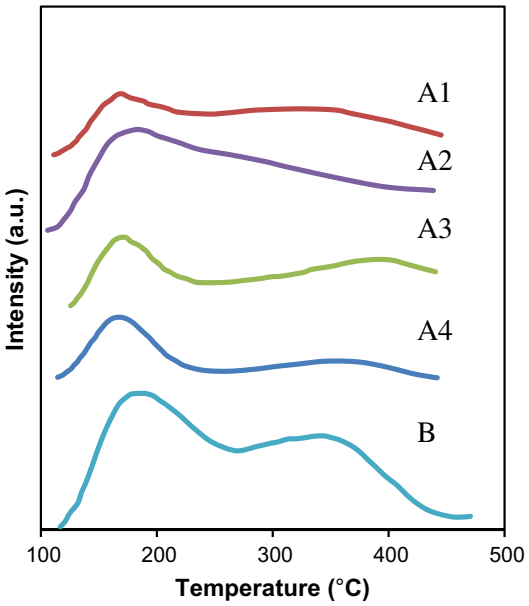

Fig. 4. NH_3-TPD of the (H)Al-RUB-41 samples A1, A2, A3, A4, and B.

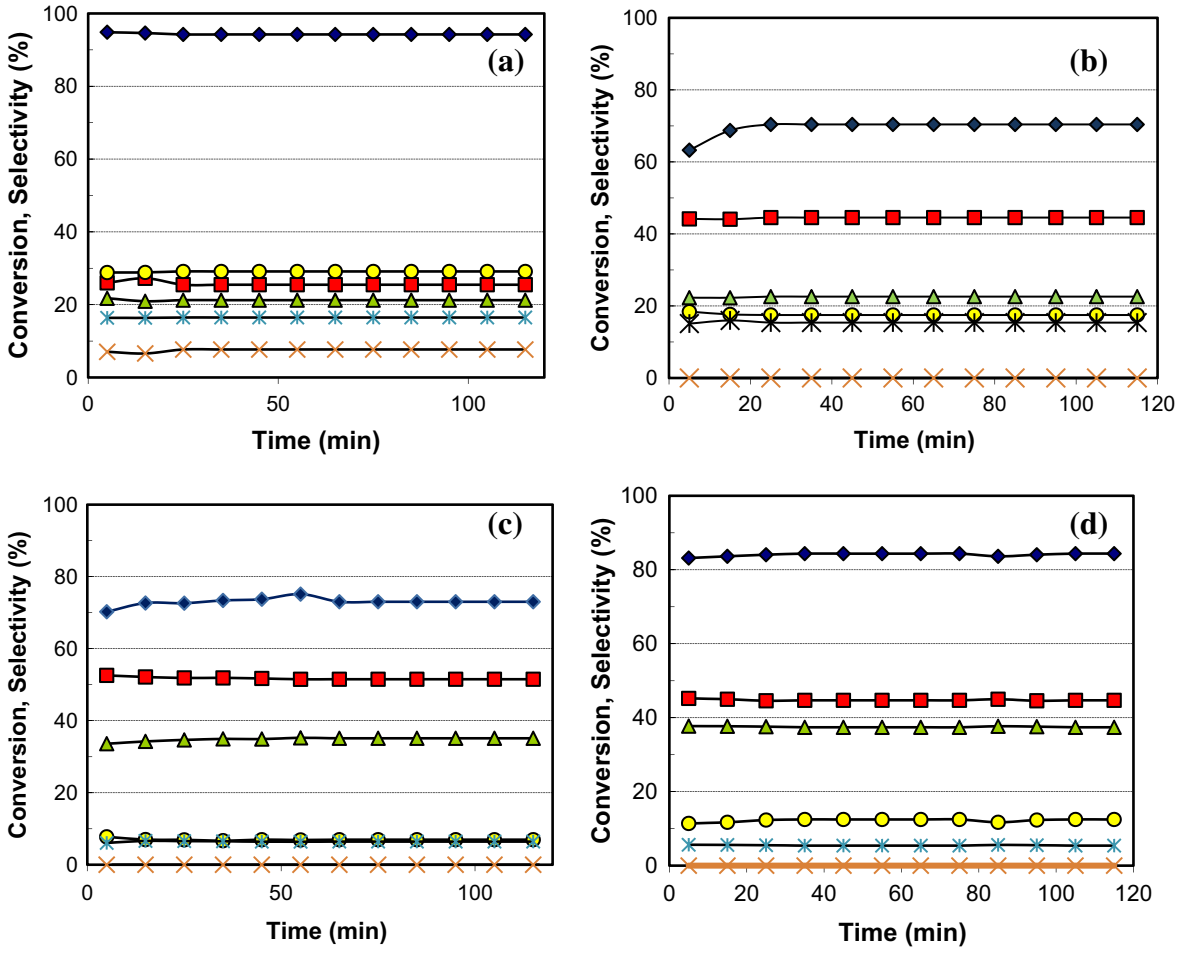

Fig. 5. Conversion and selectivity for (a) Al-MCM-41, (b) H-ZSM-5, (c) H-chabazite, (d) (H)Al-RUB-41 sample A4 in the methanol amination reaction at 340 °C, WHSV 0.66 h^{-1}, 22.5 kPa NH_3, and 11.25 kPa MeOH, (◆ = methanol conversion; selectivities based on methanol for MMA = ■; for DMA = ▲; for TMA = ●; for dimethylether = ×; for methane = ✱).

a H-ZSM-5 sample (Si/Al = 20), H-chabazite (Si/Al = 16), and (H)Al-RUB-41 (Si/Al = 163) (Fig. 5).

Since Al-MCM-41 contains mesopores which are too large to sterically hinder the production of TMA, the selectivity to TMA is high. The product distribution was close to the thermodynamic equilibrium. At 340 °C and N/C = 2, thermodynamic equilibrium is 39% TMA, 36% DMA, and 25% MMA [10]. Besides methylamines, methane and dimethylether were formed as side products. Dimethylether (DME) formation has previously been ascribed to weak acid sites [25]. As part of the methanol is used for DME formation, the actual ratio of NH_3 versus available methanol is increased, and this explains the relatively high preference for MMA within the methylamine fraction.

ZSM-5 does not allow to reach a high degree of shape selectivity either. ZSM-5 contains medium-sized 10-ring pores which are also too big to hinder the TMA production. Consequently, a relatively high selectivity for TMA was obtained, although the selectivity to MMA + DMA was enhanced and the production of TMA reduced in comparison with the MCM-41 experiment.

Chabazite, a small pore zeolite containing cages with 8-membered windows, was previously introduced as a selective amination catalyst [12]. Chabazite proved indeed highly shape selective and produced only small amounts of TMA, with MMA and DMA as the principal amination products.

Finally, comparing (H)Al-RUB-41 with ZSM-5 and Al-MCM-41, a remarkably low TMA selectivity was observed for (H)Al-RUB-41. The activity is high and was in this setup comparable to that of the ZSM-5 sample under study. At comparable methanol conversions of 70–80%, selectivities for DMA and for TMA were practically the same on ZSM-5; but on (H)Al-RUB-41, DMA selectivity was three times larger than TMA selectivity. The combined (MMA + DMA) selectivity in the methylamines fraction fluctuated in the 87–90% range during the reaction run, with only 10–13% of TMA produced. Comparing the selectivities to the different reaction products of (H)Al-RUB-41 with those of chabazite and ZSM-5, the selectivity of RUB-41 to MMA + DMA is in between that of ZSM-5 and chabazite, which correlates with the fact that the average pore size of RUB-41 is in between the pore size of ZSM-5 and chabazite. As mentioned previously, the 10-membered ring is distorted, and therefore, its dimensions are hardly larger than those of the RUB-41 8-membered ring. Therefore, the pore structure of Al-RUB-41 is not as spacious as in other 10 MR zeolites and bears similarities to that of a 8 MR zeolite [8].

The steady-state reaction data obtained with Al-RUB-41 sample A4 as a catalyst at 300 °C and 340 °C for different MeOH to NH_3 ratios were determined after 120 min on stream and are reported in Table 2. With the same NH_3/CH_3OH ratio, a higher reaction temperature results in a higher conversion of MeOH. The selectivity for methane formation increases as well, but remains within acceptable limits ($\leqslant$12%). The selectivity for TMA also increases. The obvious reason is that apparent activation energies for diffusion are always lower than the true activation energy of

Table 2
Steady-state catalytic data after 120 min time-on-stream for (H)Al-RUB-41 and a reference mordenite in the methanol amination reaction.

Catalyst	T (°C)	NH_3/CH_3OH	Conversion (%)	Selectivity (%)				
				MMA	DMA	TMA	DME	CH_4
A4	340	2:1	82	47	38	10	0	5
	340	1:1	51	44	20	24	0	12
	300	2:1	52	48	38	6	0	8
	300	1:1	42	43	42	10	0	5
H-MOR-20-M	360	1:1	87	31	61	6	2	n.g. [25]

the chemical transformation, which makes diffusional limitations more prominent at higher temperatures. Thus, at higher temperature, the reaction is gradually driven out of the pores toward the unselective outer surface. This underlines the importance of having a sufficient density of active sites inside the pores. When the NH_3/CH_3OH ratio is increased, the selectivity to TMA decreases and the methanol conversion increases. This decrease in TMA selectivity is explained by the kinetics of a set of consecutive reactions. The conversion based on methanol increases because less methanol is present in comparison with the available ammonia. No dimethylether was detected, which is in agreement with the availability of strong acid sites on this sample with Si/Al = 163. In Table 2, the catalytic data for a silylated H-Mordenite sample are included for comparison [25]. Due to the silylation treatment, the pores of mordenite are narrowed, and this results in a high selectivity for MMA and DMA, with TMA selectivity as low as 6% even at a NH_3/MeOH ratio of 1 and at high methanol conversion. Considering the results of Fig. 5 and Table 2, it can be concluded that Al-RUB-41 sample A4 is shape selective in the amination of methanol with NH_3, although higher selectivities can be reached with either chabazite or a specially modified mordenite.

3.2.2. Influence of calcination

Al-RUB-41 is formed from the layered precursor Al-RUB-39 by means of a deep calcination step. In Fig. 6, the effect of the calcination treatment on the catalyst's activity and the product distribution are reported. The as-synthesized sample is active, but results in a different product distribution in comparison with the calcined Al-RUB-41. As mentioned before, Al-RUB-41 is built from precursor Al-RUB-39 layers that condense upon calcination, while the layered Al-RUB-39 has no pore system itself. Therefore, shape selectivity is absent for Al-RUB-39. The Al-RUB-39 precursor is unselective, whereas (H)Al-RUB-41 has a high selectivity for MMA and DMA. This clearly signifies that the selective amination reaction to MMA and DMA primarily takes place inside the Al-RUB-41 pores.

3.2.3. Influence of aluminum content of RUB-41 on activity and selectivity

Several RUB-41 zeolites were prepared with different amounts of incorporated aluminum, all starting from Al isopropoxide as the Al source. Fig. 7 gives an overview of the catalytic activities and product selectivities depending on the aluminum content, reflecting the significant impact of the aluminum content on the catalyst's performance. For lower Si/Al ratios, both the activity and the selectivity to monomethylamine and dimethylamine are relatively low. Samples with higher Si/Al ratios were more active and more selective to MMA and DMA. The difference in activity can be ascribed to the stronger acid sites present in the catalysts with higher Si/Al ratios, as was evidenced by the ammonia TPD results. Another influencing factor might be the distribution of the acid sites in the lattice. In view of the structure of Al-RUB-41, more aluminum in the structure may result in an increased number of active sites on the external surface. These surface sites are unselective and hence result in a lower selectivity to MMA and DMA products.

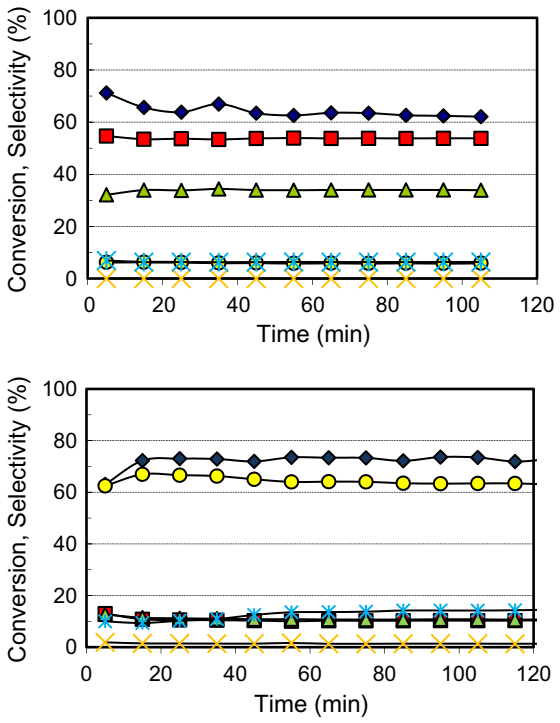

Fig. 6. Conversion and selectivity of (top) (H)Al-RUB-41 and (bottom) (H)Al-RUB-39 in the methanol amination reaction at 300 °C, WHSV 0.66, 22.5 kPa NH_3, and 11.25 kPa MeOH, (◆ = methanol conversion; selectivities for MMA = ■; for DMA = ▲; for TMA = ○; for dimethylether = ×; for methane = ✱).

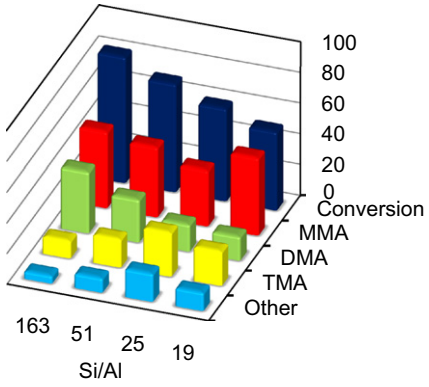

Fig. 7. Influence of Si/Al ratio of (H)Al-RUB-41 on product selectivity and conversion in methanol amination. Reaction at 340 °C, WHSV 0.66 h^{-1}, 22.5 kPa NH_3, and 11.25 kPa MeOH on (H)Al-RUB-41 samples A1–A4; data after 120 min time-on-stream.

Table 3
Steady-state catalytic data after 120 min time-on-stream of RUB-41 in the methanol amination reaction.

Catalyst	T (°C)	NH_3/CH_3OH	Conversion (%)	Selectivity (%)				
				MMA	DMA	TMA	DME	CH_4
B	340	2:1	98	46	36	11	0	7
	340	1:1	96	36	42	18	0	5
	300	2:1	64	54	34	6	0	6
	300	1:1	67	45	41	10	0	4

3.2.4. Influence of aluminum source

Until now, only Al-RUB-41 samples were discussed that were synthesized using aluminum isopropoxide as aluminum source. As an alternative aluminum source in the synthesis of Al-RUB-41 sample B, sodium aluminate was used. Al-RUB-41 sample B contains more aluminum than sample A4, a sample that was synthesized with aluminum isopropoxide and which was found to be one of the most selective and active RUB-41 samples of all samples that were synthesized with aluminum isopropoxide. According to Fig. 3, this sample has the highest concentration of strong acid sites and hence may explain the high selectivity and activity. In Table 3, the steady-state catalytic data of (H)Al-RUB-41 sample B in the amination reaction are presented. Sample B is highly active and is shape selective. At 340 °C, methanol conversion is 98%. The selectivity to MMA and DMA is consistently high, even at this high conversion. Use of sodium aluminate is hence a viable method to introduce aluminum in the structure and results in highly active and selective catalysts.

3.2.5. Influence of silylation on product selectivity

Al-RUB-41 consists of a layered structure and has a large external surface. To appreciate the amount of TMA formed on the external surface, the catalyst was treated with HMDS, a silylating agent. As the molecular dimensions of HMDS are too large to enter the pore system, only sites on the external surface are silylated. This silylation procedure should deactivate the non-selective sites and should improve the selectivity for MMA and DMA (Fig. 8). To examine the possibility to further increase the selectivity, catalyst A4 which already possesses the highest selectivity to MMA + DMA was selected and subjected to a silylation treatment. The selectivity for TMA of the untreated sample amounts to 8%; this could be reduced by silylation to 1.5%, albeit at a somewhat lower conversion. Possibly, part of the pore mouths may be blocked, leading to a lower activity. Similar phenomena have been observed when it was attempted to selectivate a medium pore zeolite like ZSM-5 by silylation [26]. Mordenite with its larger pores is hardly or even not at all sensitive to such pore blocking upon silylation [25].

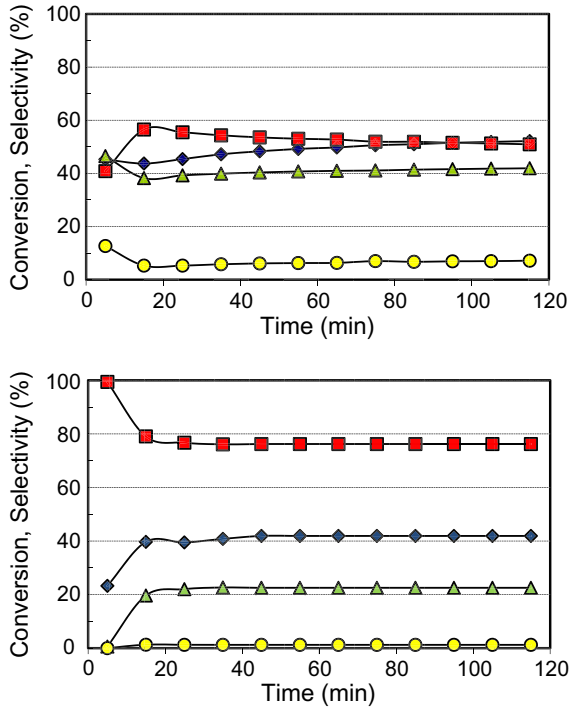

Fig. 8. Influence of silylation with HMDS on product distribution and conversion at 300 °C, WHSV 0.66, 22.5 kPa NH_3, and 11.25 kPa MeOH (◆ = methanol conversion; selectivities (%) for MMA = ■; for DMA = △; for TMA = ○) on (H)Al-RUB-41 catalysts. Top (H)Al-RUB-41 sample A4, bottom (H)Al-RUB-41 sample A4 silylated.

4. Conclusion

Al-RUB-41 materials were prepared containing varying amounts of aluminum. The introduction of aluminum in the structure was demonstrated by Al-MAS-NMR, while the structural integrity of the Al-RUB-41 was proven by XRD and SEM characterization. The catalytic activity and the shape selectivity of Al-RUB-41 were studied in the methanol amination. Al-RUB-41 enhances the production of MMA and DMA, whereas the thermodynamics of the methylamine synthesis favors the production of TMA. Catalytic experiments showed that the highest conversion and selectivity could be attained with Al-RUB-41 samples that contain low quantities of aluminum. A possible explanation could be the differences in arrangement of the aluminum in the zeolite structure, with higher aluminum contents resulting in more unselective sites, possibly due to the creation of acid sites at the outer surface. Also the synthesis of Al-RUB-41 synthesized from Na aluminate was presented, and the material was found to be highly active and selective. To further enhance the selectivity to MMA and DMA, Al-RUB-41 was treated with HMDS and a decrease in TMA formation was observed.

Acknowledgments

We are grateful to BASF AG for support in the INCOE framework. B.T. is grateful to IWT (Institute for the Promotion of Innovation by Science and Technology in Flanders).

References

[1] B. Yilmaz, U. Müller, Top. Catal. 52 (2009) 888–895.
[2] R. Millini, G. Perego, W.O. Parker Jr., G. Bellussi, L. Carluccio, Micropor. Mater. 4 (1995) 221.
[3] B. Marler, M.A. Camblor, H. Gies, Micropor. Mesopor. Mater. 910 (2006) 87.
[4] T. Ikeda, Y. Oumi, Y. Akiyama, A. Kawai, F. Mizukami, Angew. Chem. Int. Ed. 43 (2004) 4982.
[5] S. Zanardi, A. Alberti, G. Cruciani, A. Corma, V. Fornés, M. Brunelli, Angew. Chem. Int. Ed. (2004) 4933.
[6] T. Ikeda, Y. Oumi, T. Takeoka, T. Yokoyama, T. Sano, T. Hanaoka, Micropor. Mesopor. Mater. 110 (2008) 488–500.
[7] Y.X. Wang, H. Gies, B. Marler, Chem. Mater. 17 (2005) 43–49.
[8] B. Tijsebaert, C. Varszegi, H. Gies, F.-S. Xiao, X. Bao, T. Tatsumi, U. Müller, D. De Vos, Chem. Commun. (2008) 2480–2482.

[9] A.B. van Gysel, W. Musin, in: B. Elvers, S. Hawkins, G. Schultz (Eds.), Ullmann's Encyclopedia of Industrial Chemistry, fifth ed., vol. A16, VCH, Weinheim, 1990, p. 535.
[10] D.R. Corbin, S. Schwarz, G.C. Sonnichsen, Catal. Today 37 (1997) 71–102.
[11] C. Gründling, G. Eder-Mirth, J.A. Lercher, J. Catal. 160 (1996) 299–308.
[12] H.-Y. Jeon, C.-H. Shin, H.J. Jung, S.B. Hong, Appl. Catal. A 305 (2006) 70–78.
[13] S. Schwarz, D.R. Corbin, G.C. Sonnichsen, Micropor. Mesopor. Mater. 22 (1998) 409–418.
[14] F. Fetting, U. Dingerdissen, Chem. Eng. Technol. 15 (1992) 202–212.
[15] I. Mochida, A. Yasutake, H. Fujitsu, K. Takeshita, J. Catal. 82 (1983) 313–321.
[16] L.H. Callanan, C.T. O'Connor, E. van Steen, Micropor. Mesopor. Mater. 35–36 (2000) 163–172.
[17] V.A. Veefkind, C. Grundling, J.A. Lercher, J. Mol. Catal. A 134 (1998) 111–119.
[18] L. Abrams, D.R. Corbin, M. Keane, J. Catal. 126 (1990) 610–618.
[19] M.C. Ilao, H. Yamamoto, K. Segawa, J. Catal. 161 (1996) 20–30.
[20] A. Corma, J.L. Jordá, M.T. Navarro, J. Pérez-Pariente, F. Rey, J. Tsuji, Stud. Surf. Sci. Catal. 129 (2000) 169–178.
[21] B. Pauwels, G. Van Tendeloo, C. Thoelen, W. Van Rhijn, P.A. Jacobs, Adv. Mater. 13 (2001) 1317–1320.
[22] W.P. Zhang, D. Ma, X.W. Han, X.M. Liu, X.H. Bao, X.W. Guo, X.S. Wang, J. Catal. 188 (1999) 393.
[23] J.A. van Bokhoven, D.C. Koningsberger, P. Kunkeler, A.P.M. Kentgens, J. Am. Chem. Soc. 122 (2000) 12842.
[24] X.J. Li, W.P. Zhang, S.L. Liu, L.Y. Xu, X.W. Han, X.H. Bao, J. Catal. 250 (2007) 55.
[25] V.A. Veefkind, C. Gründling, J.A. Lercher, J. Mol. Catal. A 134 (1998) 111–119.
[26] S.H. Zheng, A. Jentys, J.A. Lercher, J. Catal. 241 (2006) 304–311.